Synthesis, Structures, and Polymerization Behavior of Disilane-Bridged and Bis(disilane)-Bridged [2]Ruthenocenophanes

James M. Nelson, Alan J. Lough, and Ian Manners*

Department of Chemistry, University of Toronto, 80 St. George Street, Toronto M5S 1A1, Ontario, Canada

Received May 13, 1994[⊗]

The disilane-bridged [2]ruthenocenophane $Ru(\eta\text{-}C_5H_4SiMe_2)_2$ (**6**) was synthesized via the reaction of *cis*-$RuCl_2(DMSO)_4$ with the dilithium salt $Li_2[C_5H_4SiMe_2]_2$ in THF. In order to investigate the strain present in **6** the molecular structure was determined by single crystal X-ray diffraction. The tilt angle between the planes of the cyclopentadienyl ligands in **6** (7.8(5)°) indicated that the degree of strain present is significantly less than for other [*n*]-metallocenophanes which undergo ring-opening polymerization where the tilt angles are generally 19° or greater. Significantly, the Si—Si bond in **6** was elongated to a value of 2.370(2) Å compared to a typical Si—Si bond length of 2.34 Å and this appears to provide a mechanism for the relief of strain. Compound **6** was found to be resistant to thermal ring-opening polymerization up to 350 °C. This behavior contrasts with that of hydrocarbon-bridged [2]ruthenocenophanes which readily thermally polymerize. The analogous bis(silane)-bridged [2][2]ruthenocenophane $Ru\{\eta\text{-}C_5H_3(SiMe_2)_2\}_2$ (**7**) was prepared in a manner similar to that for **6** using $Li_2[C_5H_3(SiMe_2)_2]_2$. An X-ray diffraction study of **7** indicated that this compound is significantly more strained than **6**, with a tilt angle of 12.9(2)°. The Si—Si bond in **7** (2.363(1) Å) is also elongated relative to a typical Si—Si bond, but less so than in **6**. Even though compound **7** was more strained than **6**, this species was also found to be resistant to thermal ring-opening polymerization. Crystals of **6** are monoclinic, space group $P2_1/n$, with a = 12.5407(12) Å, b = 8.3877(8) Å, c = 14.9848(9) Å, β = 109.197(6)°, V = 1488.6(2) Å^3, and Z = 4. Crystals of **7** are monoclinic, space group $C2/c$, with a = 10.908(2) Å, b = 13.605(3) Å, c = 14.859(3) Å, β = 109.89(2)°, V = 2073.6(10) Å^3, and Z = 4.

Introduction

The development of new synthetic routes to soluble, high molecular weight, and well-defined transition-metal based polymers represents an area of considerable current interest as a result of the unusual physical and chemical properties exhibited by these materials.[1–3] In 1992 we reported the discovery that strained, silicon-bridged [1]ferrocenophanes such as **1** undergo thermal

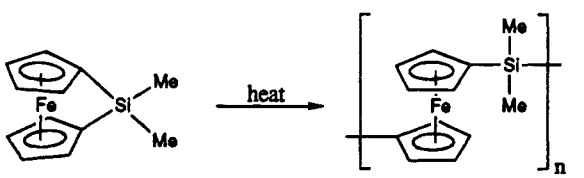

1 **2**

ring-opening polymerization (ROP) to yield the first examples of high molecular weight poly(ferrocenylsilanes) (e.g. **2**).[4] Subsequent work has shown that the ROP of [1]ferrocenophanes is quite general and provides a versatile route to a variety of metallocene-based polymers which contain silicon or alternatively other elements in the main chain structure.[5–10] Several of the [1]ferrocenophane monomers have been studied crystallographically and have been found to possess

[⊗] Abstract published in *Advance ACS Abstracts,* August 1, 1994.

(1) See, for example; (a) Dembek, A. A.; Fagan, P. J.; Marsi, M. *Macromolecules* **1993**, *26*, 2992. (b) Fyfe, H. B.; Mlekuz, M.; Zargarian, D.; Taylor, N. J.; Marder, T. B. *J. Chem. Soc., Chem. Commun.* **1991**, 188. (c) Allcock, H. R.; Dodge, J. A.; Manners, I.; Riding, G. H. *J. Am. Chem. Soc.* **1991**, *113*, 9596. (d) Wright, M. E.; Sigman, M. S. *Macromolecules* **1992**, *25*, 6055. (e) Roesky, H. W.; Lücke, M. *Angew. Chem., Int. Ed. Engl.* **1989**, *28*, 493. (f) Davies, S. J.; Johnson, B. F. G.; Khan, M. S.; Lewis, J. *J. Chem. Soc., Chem. Commun.* **1991**, 187. (g) Tenhaeff, S. C.; Tyler, D. R. *J. Chem. Soc., Chem. Commun.* **1989**, 1459. (h) Sturge, K. C.; Hunter, A. D.; McDonald, R.; Santarsiero, B. D. *Organometallics* **1992**, *11*, 3056. (i) Bayer, R.; Pohlmann, T.; Nuyken, O. *Makromol. Chem. Rapid Commun.* **1993**, *14*, 359. (j) Brandt, P. F.; Rauchfuss, T. B. *J. Am. Chem. Soc.* **1992**, *114*, 1926. (k) Gilbert, A. M.; Katz, T. J.; Geiger, W. E.; Robben, M. P.; Rheingold, A. L. *J. Am. Chem. Soc.* **1993**, *115*, 3199. (l) Nugent, H. M.; Rosenblum, M.; Klemarczyk, P. *J. Am. Chem. Soc.* **1993**, *115*, 3848.

(2) (a) Patterson, W. J.; Marus, S.; Pittman, C. H. *J. Polym. Sci. A* **1974**, *12*, 837. (b) Neuse, E. W.; Bednarik, L. *Macromolecules* **1979**, *12*, 187. (c) Gonsalves, K.; Zhanru, L.; Rausch, M. V. *J. Am. Chem. Soc.* **1984**, *106*, 3862.

(3) (a) Sheats, J. E.; Carraher, C. E.; Pittman, C. U. *Metal Containing Polymer Systems*; Plenum: New York, 1985. (b) *Inorganic and Organometallic Polymers*; Zeldin, M., Wynne, K., Allcock, H. R., Eds.; ACS Symposium Series 360; American Chemical Society: Washington DC 1988. (c) *Inorganic Polymers*; Mark, J. E., Allcock, H. R., West, R., Eds.; Prentice Hall: Englewood Cliffs, NJ, 1992. (d) Allcock, H. R. *Adv. Mater.* **1994**, *6*, 106. (e) Manners, I. *J. Chem. Soc. Ann. Rep. Prog. Chem. A* **1991**, 77. (f) Manners, I. *Ibid.* **1992**, 93. (g) Rosenblum, M. *Adv. Mater.* **1994**, *6*, 159.

(4) Foucher, D. A.; Tang, B. Z., Manners, I. *J. Am. Chem. Soc.* **1992**, *114*, 6246.

(5) (a) Foucher, D. A.; Manners, I. *Makromol. Chem., Rapid Commun.* **1993**, *14*, 63. (b) Foucher, D. A.; Ziembinski, R.; Tang, B. Z.; Macdonald, P. M.; Massey, J.; Jaeger, R.; Vancso, G. J.; Manners, I. *Macromolecules* **1993**, *26*, 2878. (c) Foucher, D. A.; Honeyman, C.; Nelson, J. M.; Tang, B. Z.; Manners, I. *Angew. Chem., Int. Ed. Engl.* **1993**, *32*, 1709. (d) Manners, I. *J. Inorg. Organomet. Polym.* **1993**, *3*, 185.

(6) Finckh, W.; Tang, B. Z.; Foucher, D. A.; Zamble, D. B.; Ziembinski, R.; Lough, A.; Manners, I. *Organometallics* **1993**, *12*, 823.

(7) Rulkens, R.; Lough, A. J.; Manners, I. *J. Am. Chem. Soc.* **1994**, *116*, 797.

0276-7333/94/2313-3703$04.50/0

strained structures in which the planes of the cyclopentadienyl ligands are substantially tilted by ca. 18–27° with respect to one another.[6,11,12] In contrast, the [2]ferrocenophane **3** containing a disilane bridge is sig-

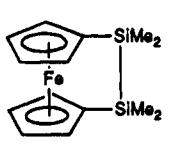

3

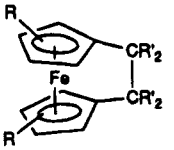

4

a R = H, R' = H
b R = Me, R' = H
c R = H, R' = Me

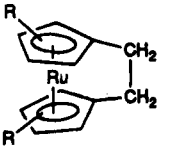

5

a R = H
b R = Me

nificantly less strained with a tilt angle of only 4.19(2)° and this species appears to be resistant to ROP.[6] However, [2]ferrocenophanes which possess smaller carbon atoms in the bridge such as the hydrocarbon-bridged species **4** are significantly more strained (tilt angles 21–23°) and these have been found to undergo ROP at elevated temperatures to yield poly(ferrocenylethylenes).[13] Very recently we reported that the formal replacement of the iron atom in **4** by a larger ruthenium atom yields hydrocarbon-bridged ruthenocenophanes **5** which possess even more strained structures with ring-tilt angles of 29–30°.[14] These species undergo ROP to yield poly(ruthenocenylethylenes).[14] In this paper we describe our attempts to increase the strain present and hence polymerizability of disilane-bridged ferrocenophanes such as **3** via the synthesis of related species in which the iron atom is replaced by ruthenium.

Results and Discussion

In contrast to their iron analogues, very few [*n*]-ruthenocenophanes have been prepared to date and, until the recent synthesis of the [2]ruthenocenophanes **5a** and **5b**,[14] none with fewer than three bridging atoms had been reported. The previously described hydrocarbon-bridged [3]- and [4]ruthenocenophanes $Ru(\eta\text{-}C_5H_4)_2(CH_2)_x$ (x = 3 or 4) were synthesized from ruthenocene via a multistep cyclization procedure and were found to possess structures with tilt angles of 14.7(2) and 1.7(2)°, respectively.[15] We used the reaction of $Li_2[C_5H_3RCH_2]_2$ (R = H or Me) with the ruthenium(II) complex *cis*-$RuCl_2(DMSO)_4$ to successfully prepare the highly strained and polymerizable species **5a** and **5b**. In order to prepare the species **6**, the disilane-bridged analogue of **5a**, we therefore used an analogous synthetic procedure.

Synthesis and Characterization of the Disilane-Bridged [2]Ruthenocenophane 6. The disilane-bridged [2]ruthenocenophane **6** was prepared in 50% yield as a very pale-yellow, sublimable crystalline

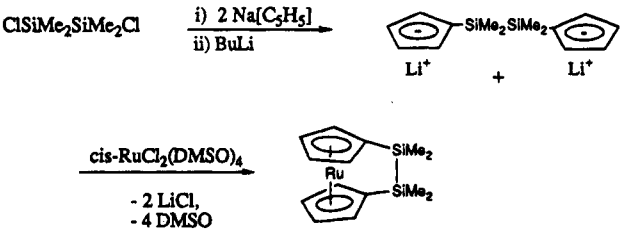

6

material by reaction of the dilithium salt $Li_2[C_5H_4SiMe_2]_2$ with the ruthenium(II) complex *cis*-$RuCl_2(DMSO)_4$. Synthesis of $Li_2[C_5H_4SiMe_2]_2$ was achieved via the reaction of $Na[C_5H_5]$ with the dichlorodisilane $ClMe_2SiSiMe_2Cl$[16] followed by deprotonation of the product with *n*-BuLi. The dichlorodisilane $ClMe_2SiSiMe_2Cl$ was prepared in two high yield steps from Me_3SiCl.[17]

The identity of **6** was confirmed by ^1H, ^{13}C, and ^{29}Si NMR, mass spectrometry, and elemental analysis which gave data consistent with the assigned structure. Significantly, the ^{13}C NMR spectroscopic data for **6** suggested that this species is not very strained. Thus the resonance for the cyclopentadienyl carbon atom bonded to silicon in **6** occurs at 71.0 ppm (in $CDCl_3$), which is similar to that found in the analogous [2]ferrocenophane **3** (72.4 ppm) and the species $Fe(\eta\text{-}C_5H_4SiMe_3)_2$ (72.1 ppm) in which the bridge between the cyclopentadienyl ligands is absent.[11f] This contrasts dramatically with the situation in strained [1]ferrocenophanes with silicon in the bridge (such as **1**) where this resonance is shifted upfield and occurs at 30–35 ppm.[6,11f] Further evidence for a relatively unstrained structure for **6** is provided by UV/visible spectroscopy. The UV/visible spectrum of **6** (in THF) in the region 250–800 nm showed absorptions at 318 nm (ϵ = 232 M^{-1} cm^{-1}), which has been assigned to $^1A_{1g} \rightarrow a^1E_{1g}$ and $^1A_{1g} \rightarrow {}^1E_{2g}$ transitions, and at 266 nm (ϵ = 290 M^{-1} cm^{-1}), assigned to a $^1A_{1g} \rightarrow b^1E_{1g}$ transition. This UV/visible spectrum is very similar to that for ruthenocene which shows two bands at 322 nm (ϵ = 200 M^{-1} cm^{-1}, $^1A_{1g} \rightarrow a^1E_{1g}$ and

(8) (a) Manners, I. *Adv. Mater.* **1994**, *6*, 68. (b) Foucher, D. A.; Ziembinski, R.; Petersen, R.; Pudelski, J.; Edwards, M.; Massey, J.; Jaeger, R.; Vancso, G. J.; Manners, I. *Macromolecules* **1994**, *27*, 3992.

(9) For the work of other groups on poly(ferrocenylsilanes) and related polymers see: (a) Rosenberg, H. U.S. Patent 3,426,053, 1969. (b) Neuse, E. W.; Rosenburg, H. *J. Macromol. Sci. Rev., Macromol. Chem.* **1970**, *C4* (1), 110–111. (c) Withers, H. P.; Seyferth, D.; Fellmann, J. D.; Garrou, P. Martin, S. *Organometallics* **1982**, *1*, 1283. (d) Tanaka, M.; Hayashi, T. *Bull. Chem. Soc. Jpn.* **1993**, *66*, 334. (e) Nguyen, M. T.; Diaz, A. F.; Dement'ev, V. V.; Pannell, K. H. *Chem. Mater.* **1993**, *5*, 1389.

(10) ROP has been previously established for a variety of organosilicon rings. See, for example: (a) Cypryk, M.; Gupta, Y.; Matyjaszewski, K. *J. Am. Chem. Soc.* **1991**, *113*, 1046. (b) Sargeant, S. J.; Zhou, S. Q.; Manuel, G.; Weber, W. P. *Macromolecules* **1992**, *25*, 2832. (c) West, R.; Hayase, S.; Iwahara, T. *J. Inorg. Organomet. Polym.* **1991**, *1*, 545. (d) Suzuki, M.; Obayashi, T.; Saegusa, T. *J. Chem. Soc., Chem. Commun.* **1993**, 717. (e) Wu, H. J.; Interrante, L. V. *Chem. Mater.* **1989**, *1*, 564. (f) Suzuki, M.; Obayashi, T.; Saegusa, T. *J. Chem. Soc., Chem. Commun.* **1993**, 717.

(11) (a) Stoeckli-Evans, H.; Osborne, A. G.; Whiteley, R. H. *Helv. Chim. Acta* **1976**, *59*, 2402. (b) Stoeckli-Evans, H.; Osborne, A. G.; Whiteley, R. H. *J. Organomet. Chem.* **1980**, *194*, 91. (c) Seyferth, D.; Withers, H. P. *Organometallics* **1982**, *1*, 1275. (d) Butler, I. R.; Cullen, W. R.; Einstein, F. W. B.; Rettig, S. J.; Willis, A. J. *Organometallics* **1983**, *2*, 128. (e) Fischer, A. B.; Bruce, J. A.; McKay, D. R.; Maciel, G. E.; Wrighton, M. S. *Inorg. Chem.* **1982**, *21*, 1766. (f) Osborne, A. G.; Whiteley, R. H.; Meads, R. E. *J. Organomet. Chem.* **1980**, *193*, 345.

(12) The cyclopentadienyl rings in ferrocene are parallel to one another. See: Dunitz, J. D.; Orgel, L. E.; Rich, A. *Acta. Crystallogr.* **1956**, *9*, 373.

(13) Nelson, J. M.; Rengel, H.; Manners, I. *J. Am. Chem. Soc.* **1993**, *115*, 7035.

(14) Nelson, J. M.; Lough, A. J.; Manners, I. *Angew. Chem., Int. Ed. Engl.* **1994**, *33*, 989.

(15) (a) Kamiyama, S.; Suzuki, T. M.; Kimura, T.; Kasahara, A. *Bull. Chem. Soc. Jpn.* **1978**, *51*, 909. (b) Ohba, S.; Saito, Y.; Kamiyama, S.; Kasahara, A. *Acta Crystallogr.* **1984**, *C40*, 53. (c) For a review of metallocenophanes see: Mueller-Westerhoff, U. T. *Angew. Chem., Int. Ed. Engl.* **1986**, *25*, 702.

(16) Jutzi, P.; Krallmann, R.; Wolf, G.; Neumann, B.; Stammler, H. G. *Chem. Ber.* **1991**, *124*, 2391.

(17) Ishikawa, M.; Kumada, M.; Sakurai, H. *J. Organomet. Chem.* **1970**, *23*, 63.

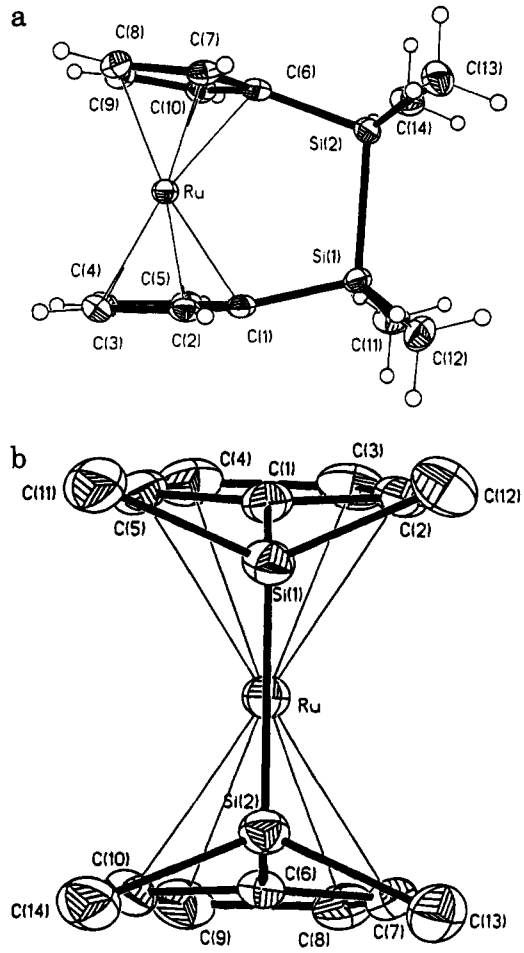

Figure 1. (a) Molecular structure of **6** (vibrational ellipsoids at the 25% probability level). (b) Alternative view of **6** (vibrational ellipsoids at the 25% probability level).

$^1A_{1g} \rightarrow {}^1E_{2g}$) and at 273 nm ($\epsilon$ = 150 M^{-1} cm^{-1}, $^1A_{1g} \rightarrow b^1E_{1g}$).[18] In contrast, the longer wavelength bands of strained, ring-tilted [1]ferrocenophanes experience a bathochromic shift of ca. 30–40 nm and increase in intensity relative to those of their unstrained analogues. For example, the long wavelength band in the UV/visible spectrum of **1** (in hexanes) occurs at 478 nm (ϵ = 240 M^{-1} cm^{-1}) compared to that of ferrocene which is at 440 nm (ϵ = 90 M^{-1} cm^{-1}).[11f]

In order to provide further data to enable us to probe the relationship between the structure and polymerization behavior of metallocenophanes and because only one [2]ruthenocenophane[14] had been previously characterized crystallographically, the structure of **6** was determined by single-crystal X-ray diffraction.

Discussion of the X-ray Structure of 6. Very pale-yellow single crystals of **6** suitable for an X-ray diffraction study were obtained from a solution of the compound in hexanes at −20 °C. Two alternative views of the molecular structure of **6** are shown in Figure 1. A summary of cell constants and data collection parameters are included in Table 1, and the fractional coordinates and important bond lengths and angles are listed in Tables 2 and 3 for **6**. The angles α, β, and δ used in discussing the structures are defined in Figure 2.[6,11f] The values of these angles for the compounds **1a**, **3**, **4c**, **5a**, and **6**–**8** are compiled in Table 6.

(18) Gray, H. B.; Hendrickson, D. N.; Sohn, Y. S. *J. Am. Chem. Soc.* **1971**, *93*, 3603.

Table 1. Summary of Crystal Data and Intensity Collection Parameters

	6	**7**
empirical formula	$C_{14}H_{20}RuSi_2$	$C_{18}H_{30}RuSi_4$
M_r	345.6	459.9
cryst class	monoclinic	monoclinic
space group	$P2_1/n$	$C2/c$
a, Å	12.5407(12)	10.908(2)
b, Å	8.3877(8)	13.605(3)
c, Å	14.9848(9)	14.859(3)
α, deg		
β, deg	109.197(6)	109.89(2)
γ, deg		
V, Å^3	1488.6(2)	2073.6(10)
Z	4	4
D_{calc}, g cm^{-3}	1.542	1.473
μ(Mo Kα), cm^{-1}	0.19	0.098
F(000)	704	952
ω-scan width, deg	0.59 + 0.61 tan θ	0.6 θ
range θ collcd, deg	4.9–50.0	3.5–54.0
total no. of rflns	2985	2458
no. of unique rflns	2612	2245
R_{int}	3.65	2.41
no. of obsd data used [$I > 3\sigma(I)$]	1857	1234
weighting g	0.001	0.0007
R	0.032	0.023
R_w	0.043	0.034
GOF	1.02	1.04
$(\Delta/\sigma)_{max}$ in last cycle	0.00	0.08
no. of params refined	155	165
Δρ(max) in final ΔF map, e Å^{-3}	0.62	0.41

Table 2. Final Fractional Atomic Coordinates (×10^4) and Equivalent Isotropic Displacement Coefficients (Å^2 × 10^3) for the Non-Hydrogen Atoms of 6

	x	*y*	*z*	*U*(eq)[a]
Ru	0.38569(3)	0.11074(4)	0.22150(2)	0.0332(1)
Si(1)	0.5685(1)	−0.1499(2)	0.1849(1)	0.038(1)
Si(2)	0.5769(1)	−0.1531(2)	0.3452(1)	0.037(1)
C(1)	0.4595(4)	0.0037(6)	0.1239(3)	0.037(2)
C(2)	0.3382(4)	−0.0219(6)	0.0905(3)	0.040(2)
C(3)	0.2828(5)	0.1269(7)	0.0724(3)	0.051(2)
C(4)	0.3670(5)	0.2489(7)	0.0922(4)	0.053(2)
C(5)	0.4746(5)	0.1713(6)	0.1241(3)	0.044(2)
C(6)	0.4713(4)	−0.0007(6)	0.3560(3)	0.036(2)
C(7)	0.3538(4)	−0.0264(6)	0.3323(3)	0.041(2)
C(8)	0.2982(5)	0.1228(6)	0.3250(4)	0.046(2)
C(9)	0.3806(5)	0.2422(7)	0.3458(4)	0.051(2)
C(10)	0.4880(5)	0.1687(6)	0.3647(3)	0.045(2)
C(11)	0.7058(5)	−0.0883(8)	0.1738(4)	0.063(3)
C(12)	0.5232(5)	−0.3460(7)	0.1260(4)	0.059(2)
C(13)	0.5382(5)	−0.3515(6)	0.3824(4)	0.056(2)
C(14)	0.7200(5)	−0.0951(8)	0.4255(4)	0.059(2)

[a] Equivalent isotropic *U* defined as one-third of the trace of the orthogonalized U_{ij} tensor.

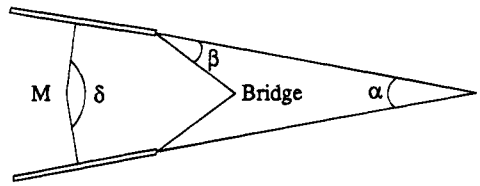

Figure 2. Distortions in metallocenophanes defining angles α, β, and δ.

The presence of a larger ruthenium atom in **6** leads to subtle rather than dramatic structural differences in comparison to the iron analogue **3**. For example, the tilt angle α between the planes of the cyclopentadienyl rings in **6** (7.8(5)°) is only ca. 3.6° greater than that in **3** (α = 4.19(2)°). The difference can be further appreciated by comparison of the Cp–M–Cp angles δ for these species. Thus, for **6** the value of δ is 174.2(2)° whereas for **3** the angle is 176.48(3)° which is closer to 180°. The

Table 3. Selected Distances (Å) and Angles (deg) for 6 (Estimated Standard Deviations (Esd's) Are in Parentheses)

Bond Distances			
Ru—C(1)	2.168(6)	Ru—C(2)	2.163(5)
Ru—C(3)	2.185(5)	Ru—C(4)	2.202(6)
Ru—C(5)	2.170(6)	Ru—C(6)	2.160(4)
Ru—C(7)	2.162(6)	Ru—C(8)	2.176(6)
Ru—C(9)	2.182(6)	Ru—C(10)	2.163(4)
Si(1)—Si(2)	2.370(2)	Si(1)—C(1)	1.882(5)
Si(1)—C(11)	1.857(7)	Si(1)—C(12)	1.865(6)
Si(2)—C(6)	1.886(5)	Si(2)—C(13)	1.869(6)
Si(2)—C(14)	1.866(5)	C(1)—C(2)	1.453(7)
C(1)—C(5)	1.418(7)	C(2)—C(3)	1.410(8)
C(3)—C(4)	1.430(9)	C(4)—C(5)	1.432(8)
C(6)—C(7)	1.414(7)	C(6)—C(10)	1.435(7)
C(7)—C(8)	1.419(8)	C(8)—C(9)	1.399(8)
C(9)—C(10)	1.422(8)		
Bond Angles			
Si(2)—Si(1)—C(11)	111.1(2)	Si(2)—Si(1)—C(1)	106.5(2)
Si(2)—Si(1)—C(12)	112.0(2)	C(1)—Si(1)—C(11)	108.2(3)
C(11)—Si(1)—C(12)	110.5(3)	C(1)—Si(1)—C(12)	108.3(2)
Si(1)—Si(2)—C(13)	112.5(2)	Si(1)—Si(2)—C(6)	106.3(2)
Si(1)—Si(2)—C(14)	111.3(2)	C(6)—Si(2)—C(13)	108.7(3)
C(13)—Si(2)—C(14)	109.2(3)	C(6)—Si(2)—C(14)	108.8(2)
Ru—C(1)—C(2)	70.2(3)	Ru—C(1)—Si(1)	111.1(2)
Ru—C(1)—C(5)	71.0(3)	Si(1)—C(1)—C(2)	125.3(4)
C(2)—C(1)—C(5)	105.7(4)	Si(1)—C(1)—C(5)	127.1(4)
Ru—C(2)—C(3)	71.9(3)	Ru—C(2)—C(1)	70.6(3)
Ru—C(3)—C(2)	70.2(3)	C(1)—C(2)—C(3)	109.2(5)
C(2)—C(3)—C(4)	108.1(5)	Ru—C(3)—C(4)	71.6(3)
Ru—C(4)—C(5)	69.7(3)	Ru—C(4)—C(3)	70.3(3)
Ru—C(5)—C(1)	70.8(3)	C(3)—C(4)—C(5)	107.1(5)
C(1)—C(5)—C(4)	109.8(5)	Ru—C(5)—C(4)	72.1(4)
Ru—C(6)—C(7)	71.0(3)	Ru—C(6)—Si(2)	111.2(2)
Ru—C(6)—C(10)	70.7(3)	Si(2)—C(6)—C(7)	125.3(4)
C(7)—C(6)—C(10)	106.4(5)	Si(2)—C(6)—C(10)	126.4(4)
Ru—C(7)—C(8)	71.5(3)	Ru—C(7)—C(6)	70.8(3)
Ru—C(8)—C(7)	70.4(3)	C(6)—C(7)—C(8)	109.2(5)
C(7)—C(8)—C(9)	107.8(5)	Ru—C(8)—C(9)	71.5(4)
Ru—C(9)—C(10)	70.2(3)	Ru—C(9)—C(8)	71.1(3)
Ru—C(10)—C(6)	70.5(2)	C(8)—C(9)—C(10)	108.4(5)
C(6)—C(10)—C(9)	108.1(5)	Ru—C(10)—C(9)	71.6(3)

structural differences are less than those between the hydrocarbon-bridged analogues **5a** and **4c**.[19] For the latter species the difference in the tilt angle α (ca. 6.6°) and the Cp—M—Cp angle δ (ca. 4.1°) is indicative of a significantly more strained structure in the case of the ruthenium complex **5a**. Similarly, the difference in the angle β between the plane of the cyclopentadienyl ligands and the C(Cp) bridging atom bonds for the disilane-bridged species **6** and **3** (ca. 1.6°) is less than that for the hydrocarbon-bridged species **5a** and **4c** (ca. 3.5°). The reason for these relatively small structural differences between **6** and **3** can be traced to the bonds within the bridge structure. In the case of **6** the Si—Si bond (2.370(2) Å) is significantly elongated in comparison to that in **3** (2.3535(9) Å). The value in the latter is only slightly greater than that for typical Si—Si bonds (ca. 2.34 Å) which are found in compounds without bridges between the cyclopentadienyl ligands such as $Fe(\eta\text{-}C_5H_4SiMe_2SiMe_3)_2$ (2.34(1) Å) and $[Fe(\eta\text{-}C_5H_5)(\eta\text{-}C_5H_4SiMe_2)]_2$ (2.340(1) Å).[20] The elongation of the Si—Si bond in **6** is accompanied by an untwisting of the bridge and an eclipsing of the cyclopentadienyl ligands relative to the situation in **3**. For example, the bridge in **6** is twisted by an angle of only 0.2(5)° with respect to the plane defined by the centroids of the cyclopentadienyl ligands and the metal atom whereas the corresponding angle in **3** is 8.4(4)°. Thus, the methyl groups attached to silicon in **6** are virtually eclipsed with C(11)—Si(1)—Si(2)—C(14) and C(12)—Si(1)—Si(2)—C(13) torsion angles of 0.6(8) and 0.6(8)°, respectively (see Figure 1b). In addition, the angle between the Cp(centroid)—C(ipso) bonds is only 0.6(7)°, which indicates that the cyclopentadienyl rings are virtually eclipsed. By comparison, in the case of **3** the methyl groups are more staggered with C(11)—Si(1)—Si(2)—C(14) and C(12)—Si(1)—Si(2)—C(13) torsion angles of 8.34(19) and 7.85(18)° and an angle between the Cp(centroid)—C(ipso) bonds projected on the mean plane of the cyclopentadienyl ligands of 6.0(1)°.

The structure of the disilane-bridged [2]ruthenocenophane **6** is also interesting to compare to that of the hydrocarbon-bridged analogue **5a**.[14] Because the covalent radius of carbon is significantly less than that of silicon, the length of the C—C bond in the bridge in **5a** is only 1.549(9) Å compared to the length of the elongated Si—Si bond in **6** (2.370(2) Å). For the same reason, the C(Cp)—C bonds in **5a** (average length 1.528(8) Å) are also shorter than the C(Cp)—Si bonds in **6** (average length 1.884(5) Å). These factors lead to a dramatic difference in tilt angle between these compounds (for **6** α = 7.8(5)° whereas for **5a** α = 29.6(5)°). Another significant difference between these species is found in the twist angles of the bridges with respect to the plane defined by the centroids of the cyclopentadienyl ligands and the metal atom. This angle is essentially zero for **6**, indicating that the cyclopentadienyl ligands are eclipsed, whereas for the hydrocarbon-bridged species **5a** the angle is 21.3(5)°. This leads to a staggering of the cyclopentadienyl rings in the latter with an angle of 8.4(5)° between the projection of the Cp(centroid)—C(ipso) bonds on the mean plane of the cyclopentadienyl ligands. This difference between **6** and **5a** is probably a consequence of the longer Si—Si bond in the former which allows sterically unfavorable eclipsing of the methyl substituents on the adjacent silicon atoms more readily than the case of the shorter C—C bond.

Polymerization Behavior of 6. Attempts to thermally polymerize **6** involved heating this species in the melt in a manner analogous to that used to successfully polymerize **5a**.[14] However, when **6** was heated in an evacuated tube at temperatures between 150 and 350 °C for 7 days, no increase in viscosity was detected and analysis of the tube contents by ^{1}H NMR showed only the presence of unreacted **6**. Subsequent analysis by GPC showed that no high molecular weight material (M_w > 1000) was present. In addition, a sealed tube containing **6** was heated for 15 min at 380 °C. This resulted in the partial decomposition of the monomer to black insoluble material. Analysis by mass spectrometry showed no evidence for the formation of even oligomeric material. As the thermal polymerization of **6** was unsuccessful, anionic ring-opening methods, which have been previously used to successfully induce the anionic ROP of cyclic tetrasilanes[10a] and recently silicon-bridged [1]ferrocenophanes such as **1**,[7] were investigated. However, when **6** was heated in the melt in the presence of a small quantity of $K[OSiMe_3]$ at 140

(19) Burke Laing, M.; Trueblood, K. N. *Acta Crystallogr.* **1965**, *19*, 373.

(20) (a) Hirotsu, K.; Higuchi, T.; Shimda, A. *Bull, Chem. Soc. Jpn.* **1968**, *41*, 1557. (b) Dement'ev, V. V.; Cervantes-Lee, F.; Parkanyi, L.; Sharma, H.; Pannell, K. H.; Nguyen, M. T. K.; Diaz, A. F. *Organometallics* **1993**, *12*, 1983. (c) The sum of the covalent radii for silicon is 2.34 Å: Stark, J. G.; Wallace, H. G. *Chemistry Data Book*; John Murray: London, 1975.

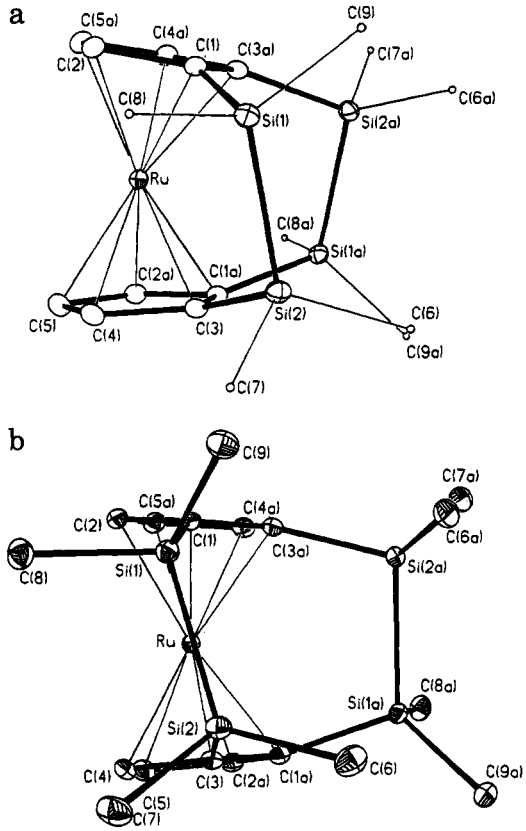

Figure 3. (a) Molecular structure of **7** (vibrational ellipsoids at the 25% probability level). (Methyl groups attached to silicon have been assigned arbitrary radii for clarity.) (b) Alternative view of **7** (vibrational ellipsoids at the 25% probability level).

or 350 °C, no signs of polymerization were detected. In all cases only unreacted **6** was detected according to ^{1}H NMR and mass spectrometry. Furthermore, GPC analysis confirmed that no material with $M_w > 1000$ had been formed.

Synthesis and Characterization of the Bis(disilane)-Bridged [2][2]Ruthenocenophane (7). The nonpolymerizability of **6** under conditions where metallocenophanes such as **1**, **4a** and **4b**, and **5a** and **5b** polymerize is probably a consequence of the relatively small amount of strain present. In order to introduce more ring tilt and hence strain in the metallocenophane, we explored the synthesis of a species **7** analogous to **6** but with two disilane bridges.

The [2][2]ruthenocenophane **7** was prepared in 50% yield as a pale yellow, sublimable crystalline material by reaction of the dilithium salt $Li_2[C_5H_3(SiMe_2)_2]_2$ with *cis*-$RuCl_2(DMSO)_4$. Synthesis of $Li_2[C_5H_3(SiMe_2)_2]_2$ was carried out by reaction of the dichlorodisilane $ClMe_2SiSiMe_2Cl$ with a THF solution of $Li_2[C_5H_4SiMe_2]_2$ followed by deprotonation with *n*-BuLi, as reported previously by Jutzi and co-workers who have used this approach to prepare the analogous [2][2]ferrocenophane **8**.[16] The identity of **7** was confirmed by ^{1}H, ^{13}C, and ^{29}Si NMR, mass spectrometry, and elemental analysis. These data were consistent with the assigned structure. In particular, the ^{1}H NMR spectrum of **7** in $CDCl_3$ (Figure 4) showed a low field triplet and a doublet resonance at 4.87 and 5.05 ppm in a 1:2 integration ratio for the two sets of protons (β and α) of the η-C_5H_3 ligand and two high field singlet resonances at 0.49 and 0.60 ppm for the protons associated with the interior and exterior methyl groups in the disilane bridges.

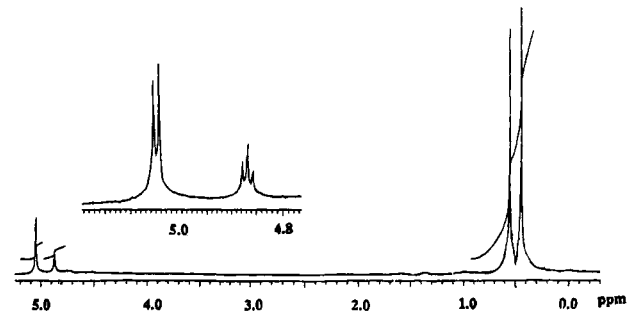

Figure 4. ^{1}H NMR spectrum of **7** (in $CDCl_3$).

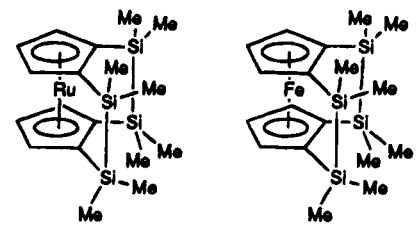

7 **8**

In a way similar to the case of **6** discussed above, the ^{13}C NMR spectroscopic data for **7** suggested that this species is not very strained. Thus, the ^{13}C NMR resonance for the cyclopentadienyl carbon atoms bonded to silicon in **7** occurs at 71.0 ppm (in $CDCl_3$), which is at a chemical shift similar to that for the unstrained, unbridged species $Fe(\eta$-$C_5H_4SiMe_3)_2$ (72.1 ppm) rather than that for the highly strained species **1** (33.5 ppm).[6] The ipso carbon ^{13}C NMR resonance for **7** also possesses a chemical shift similar to that for **8** (tilt angle = 7.2°, δ = 71.6 ppm). This indicates that relatively little structural distortion is present at the cyclopentadienyl carbon atom bonded to silicon in **7**. However, evidence for appreciable tilting of the cyclopentadienyl ligands in **7** was provided by UV/visible spectroscopy. Thus the UV/visible spectrum of **7** (in THF) in the region 250–600 nm showed absorptions at 345 nm (ϵ = 275 M^{-1} cm^{-1}, $^1A_{1g} \rightarrow a^1E_{1g}$) and 270 nm ($\epsilon$ = 280 M^{-1} cm^{-1}, $^1A_{1g} \rightarrow b^1E_{1g}$). The longer wavelength band is shifted bathochromically from that for ruthenocene at 322 nm (ϵ = 200 M^{-1} cm^{-1})[18] whereas the lower wavelength band is virtually unchanged (273 nm, ϵ = 150 M^{-1} cm^{-1}). Bathochromic shifts of up to ca. 40 nm are found for the long wavelength band for strained species such as **1** relative to their unstrained counterparts.[6,11f] In order to provide further insight into the structural distortions in **7**, a single crystal X-ray diffraction study was performed.

X-ray Structure of 7. Pale-yellow single crystals of **7** were obtained by allowing a solution of the compound in hot hexanes to cool to room temperature followed by further cooling to −20 °C. Two alternative views of the molecular structure of **7** are shown in Figure 3. A summary of cell constants and data collection parameters are included in Table 1, and the fractional coordinates and important bond lengths and angles are listed in Tables 4 and 5. The angles α, β, and δ used in discussing the structures are defined in Figure 2 and their values for **1a**, **3**, **4c**, **5a**, and **6**–**8** are compiled in Table 6.

Table 4. Final Fractional Atomic Coordinates ($\times 10^4$) and Equivalent Isotropic Displacement Coefficients (Å $\times 10^3$) for the Non-Hydrogen Atoms of 7

	x	*y*	*z*	*U*(eq)[a]
Ru	0.0000	0.3541(0)	0.2500	0.0153(1)
Si(1)	0.22024(4)	0.51853(3)	0.36655(3)	0.0182(2)
Si(2)	0.15536(5)	0.55044(4)	0.20055(3)	0.0193(2)
C(1)	0.0948(2)	0.4314(1)	0.3823(1)	0.018(1)
C(2)	0.1224(2)	0.3276(1)	0.3986(1)	0.021(1)
C(3)	0.0456(2)	0.4431(1)	0.1450(1)	0.018(1)
C(4)	0.0993(2)	0.3459(1)	0.1451(1)	0.021(1)
C(5)	−0.0034(2)	0.2756(1)	0.1186(1)	0.023(1)
C(6)	0.0795(2)	0.6725(2)	0.1578(2)	0.030(1)
C(7)	0.3035(2)	0.5445(2)	0.1638(2)	0.032(1)
C(8)	0.3752(2)	0.4464(2)	0.3941(2)	0.028(1)
C(9)	0.2547(2)	0.6251(2)	0.4517(2)	0.026(1)

[a] Equivalent isotropic *U* defined as one-third of the trace of the orthogonalized U_{ij} tensor.

Table 5. Selected Distances (Å) and Angles (deg) for 7 (Estimated Standard Deviations (Esd's) are in Parentheses)

Bond Distances			
Ru−C(1)	2.159(2)	Ru−C(2)	2.186(2)
Ru−C(3)	2.163(2)	Ru−C(4)	2.183(2)
Ru−C(5)	2.214(2)	Ru−C(1A)	2.159(2)
Ru−C(2A)	2.186(2)	Ru−C(3A)	2.163(2)
Ru−C(4A)	2.183(2)	Ru−C(5A)	2.214(2)
Si(1)−Si(2)	2.363(1)	Si(1)−C(1)	1.884(2)
Si(1)−C(8)	1.875(2)	Si(1)−C(9)	1.876(2)
Si(2)−C(3)	1.891(2)	Si(2)−C(6)	1.867(2)
Si(2)−C(7)	1.875(3)	C(1)−C(2)	1.448(2)
C(1)−C(3A)	1.453(2)	C(2)−C(5A)	1.423(3)
C(3)−C(4)	1.447(3)	C(3)−C(1A)	1.453(2)
C(4)−C(5)	1.423(3)	C(5)−C(2A)	1.423(3)
Bond Angles			
Si(2)−Si(1)−C(8)	104.6(1)	Si(2)−Si(1)−C(1)	105.9(1)
Si(2)−Si(1)−C(9)	118.8(1)	C(1)−Si(1)−C(8)	106.4(1)
C(8)−Si(1)−C(9)	107.4(1)	C(1)−Si(1)−C(9)	112.9(1)
Si(1)−Si(2)−C(6)	117.3(1)	Si(1)−Si(2)−C(3)	103.5(1)
Si(1)−Si(2)−C(7)	108.3(1)	C(3)−Si(2)−C(6)	113.4(1)
C(6)−Si(2)−C(7)	105.4(1)	C(3)−Si(2)−C(7)	108.7(1)
Ru−C(1)−C(2)	71.6(1)	Ru−C(1)−Si(1)	109.7(1)
Ru−C(1)−C(3A)	70.5(1)	Si(1)−C(1)−C(2)	121.1(1)
C(2)−C(1)−C(3A)	107.0(1)	Si(1)−C(1)−C(3A)	129.6(1)
Ru−C(2)−C(5A)	72.2(1)	Ru−C(2)−C(1)	69.5(1)
Ru−C(3)−Si(2)	112.6(1)	C(1)−C(2)−C(5A)	109.2(2)
Si(2)−C(3)−C(4)	120.6(1)	Ru−C(3)−C(4)	71.3(1)
Si(2)−C(3)−C(1A)	131.1(1)	Ru−C(3)−C(1A)	70.2(1)
Ru−C(4)−C(3)	69.8(1)	C(4)−C(3)−C(1A)	106.8(1)
C(3)−C(4)−C(5)	109.5(2)	Ru−C(4)−C(5)	72.3(1)
Ru−C(5)−C(2A)	70.1(1)	Ru−C(5)−C(4)	69.9(1)
		C(4)−C(5)−C(2A)	107.5(2)

The effect of adding another disilane bridge increases the tilt angle α from a value of 7.8(5)° in **6** to 12.9(2)° in **7**. The tilt angle in **7** is significantly greater than that in the iron analogue **8** (α = 7.2°).[16] The greater ring tilting in **7** compared to **6** can also be appreciated by comparing the Cp−M−Cp (M = Fe, Ru) angle δ for these species. Thus **7** possesses a smaller value for δ (170.8(1)°) compared to **6** (δ = 174.2(2)°). The more tilted structure of **7** is consistent with the UV/visible data for this species, which shows a significant bathchromic shift of the longer wavelength band relative to the values found in unstrained systems. In contrast to the significant (ca. 5°) difference in tilt angles between **7** and **6** the values of the angle β between the plane of the cyclopentadienyl ligands and the C(Cp) bridging atom bonds are similar. Thus for **7** β = 12.2(1) and 14.4(1)° whereas for **6** β = 12.4(3)°. Indeed, the values of β for **7** are quite similar to those for the double-strapped iron analogue **8** (β = 11.1 and 14.6°). The similarly small values for β in these compounds explains the normal chemical shift for the ^{13}C NMR resonance of **7** arising from the ipso carbon atoms of the cyclopentadienyl groups. In contrast, in [1]ferrocenophanes such as **1** where β = 37.0(6)° the ipso carbon resonance is dramatically shifted to high field. The Si−Si bond length in **7** (2.363(1) Å) is slightly shorter than that in **6** (2.370(2) Å) but is very similar to that found in the less ring-tilted iron analogue **8** (2.365(4) Å) and is again indicative of a significant elongation relative to a normal Si−Si bond (2.34 Å). The disilane bridges of **7** are considerably twisted relative to the plane containing the centroids on the cyclopentadienyl rings and the ruthenium atom. Thus the Si−Si bond makes an angle of 15.7(5)° with this plane which results in a staggering of the cyclopentadienyl ligands by an angle of 12.5(4)°. This is in sharp contrast to the situation in **6** where the Si−Si bond of the disilane bridge is essentially parallel to the plane and the corresponding angle is 0.2(5)°. The more pronounced twisting of the disilane bridges in **7** compared to the situation in **6** is probably a result of unfavorable steric interactions involving the methyl groups attached to silicon between the two bridges. The methyl groups attached to silicon in the disilane bridge of **7** are staggered with C(8)−Si(1)−Si(2)−C(7) and C(9)−Si(1)−Si(2)−C(6) torsion angles of 23.6(4) and 23.6(4)°, respectively. A similar twisting of the disilane bridges is found in the [2][2]ferrocenophane **8** where the bridge makes an angle of ca. 16.5° to the plane containing the centroids on the cyclopentadienyl rings and the iron atom. This results in a staggering of the cyclopentadienyl ligands in **8** by an angle of 13.0°.

Polymerization Behavior of 7. Attempts to thermally polymerize **7** also involved heating this species in the melt in a manner analogous to that used to successfully polymerize **5a** and **5b**. However, when **7** was heated in an evacuated tube at temperatures from 150 to 350 °C for 7 days, no increase in viscosity was detected and analysis of the tube contents by ^1H NMR showed only the presence of unreacted **7**. Subsequent analysis by GPC showed that no high molecular weight material (M_w > 1000) was present. Additionally, a sealed tube containing **7** was heated for 15 min at 380 °C, resulting in the decomposition of the monomer to black insoluble material with no detectable increase in viscosity. These results indicate that compound **7**, even though it is more strained than **6**, is still insufficiently strained to polymerize. As in the case of **6**, anionic methods of polymerization were also attempted. Sealed tubes of **7** were heated in the presence of $KOSiMe_3$ at temperatures ranging from 140 to 250 °C for 24-h periods, and the tube contents were subsequently analyzed by NMR, mass spectrometry, and GPC. Only tubes that underwent heat treatment at 250 °C showed any change, resulting in the decomposition of **7** to brown insoluble material. No evidence for the formation of any oligomeric or polymeric material derived from **7** was found by GPC or mass spectrometry.

Summary

The disilane-bridged ruthenocenophane **6** and the bis(disilane)-bridged ruthenocenophane **7** have been synthesized and characterized. Unlike hydrocarbon-bridged [2]ruthenocenophanes **5a** and **5b**, these compounds are resistant to thermal ROP. This difference in polymerization behavior can be attributed to the lower degree

Table 6. Selected Structural Data for [1]- and [2]Metallocenophanes

	1a	3	4c	5a	6	7	8[c]
Si—Si distance Å		2.3535(9)			2.370(2)	2.363(1)	2.365(4)
Fe displacement,[a] Å	0.2164(11)	0.027(3)	0.432(12)	0.321(5)	0.092(6)	0.145(2)	0.082
ring tilt, α, deg	20.8(5)	4.19(2)	23(1)	29.6(5)	7.8(5)	12.9(2)	7.2
β,[b] deg	37.0(6)	10.8(3)	10.8(10)	13.4(5)	12.4(3)	14.4(1)	11.1
			8.9(13)			12.2(1)	14.6
twist,[d] deg		8.4(4)		21.3(5)	0.2(5)	15.7(5)	16.5
Cp—Fe—Cp, δ, deg	164.74(8)	176.48(3)	163.4(6)	159.3(2)	174.2(2)	170.8(1)	174.4
ref	6	6	19	14	this work	this work	16

[a] The displacement of the iron atom from the line joining the two centroids of the cyclopentadienyl rings. [b] The angle(s) between the planes of the cyclopentadienyl ligands and the C(Cp)—E bonds (where E = bridging atom). [c] Estimated standard deviations not available (see ref 16). [d] The angle(s) between the plane defined by the centroids of the cyclopentadienyl ligands and the metal atom and the E—E bond (where E = bridging atom).

of strain present in **6** and **7**. This assertion is supported by an examination of the structures of these compounds by X-ray diffraction. The results of the crystallographic work suggest that elongation of the Si—Si bond in the bridge structure plays an important role in the relief of strain in **6** and **7**. We are now investigating the synthesis and polymerization behavior of other, potentially more strained ruthenocenophanes, and our results concerning this work will be reported in the near future.

Experimental Section

Materials. Trimethylchlorosilane, hexamethyldisilane ($Me_3SiSiMe_3$), sodium metal, potassium metal, 1.6 M butylithium in hexanes, and dicyclopentadiene were purchased from Aldrich. $RuCl_3{\cdot}xH_2O$ was provided through a generous loan from Johnson Matthey. The dichlorodisilane $ClMe_2SiSiMe_2Cl$ was prepared via the reaction of $Me_3SiSiMe_3$ with Me_3SiCl in the presence of $AlCl_3$.[17] *cis*-$RuCl_2(DMSO)_4$[21] and the dilithium salts $Li_2[C_5H_4(SiMe_2)_2]_2$ and $Li_2[C_5H_4SiMe_2]_2$[16] were synthesized by literature procedures.

Equipment. All reactions and manipulations were carried out under an atmosphere of prepurified nitrogen using either Schlenk techniques or an inert-atmosphere glovebox (Vacuum Atmospheres). Solvents were dried by standard methods, distilled, and stored under nitrogen over activated molecular sieves. ^1H NMR spectra (200 MHz) and 50.3-MHz ^{13}C NMR spectra were recorded either on a Varian Gemini 200 or a Varian XL 400 spectrometer, respectively. The 79.4-MHz ^{29}Si NMR spectra were referenced externally to $SiMe_4$ (TMS) and were recorded on a Varian XL 400 spectrometer utilizing either a normal (proton coupled) or a DEPT pulse sequence (proton decoupled) with a $^2J_{Si-H}$ coupling of 6.7 Hz. All NMR spectra were referenced internally to TMS. Mass spectra were obtained with the use of a VG 70-250S mass spectrometer operating in an electron impact (EI) mode. UV/visible spectra were recorded on a Hewlett-Packard 6452A diode array spectrophotometer using a 1-cm quartz cell. Molecular weights were estimated by gel permeation chromatography (GPC) using a Waters Associates liquid chromatograph equipped with a 510 HPLC pump, U6K injector, Ultrastyragel columns with a pore size between 10^3 and 10^5 Å, and a Waters 410 differential refractometer. A flow rate of 1.0 mL/min was used, and the eluent was a solution of 0.1% tetra-*n*-butylammonium bromide in THF. Polystyrene standards were used for calibration purposes. Elemental analyses were performed by the Canadian Microanalytical Service Ltd., Delta, BC.

Synthesis of the [2]Ruthenocenophane 6. A solution of $Li_2[C_5H_4SiMe_2]_2$ (0.303 g, 1.17 mmol) in THF (40 mL) was added dropwise to a suspension of *cis*-$RuCl_2(DMSO)_4$ (0.568 g, 1.17 mmol) in the same solvent (40 mL) at −78 °C. The reaction mixture was stirred at this temperature for 3 h and was then allowed to warm to room temperature over a 12-h period. Following solvent removal in vacuo, very pale-yellow microcrystalline **6** was isolated and purified by vacuum sublimation (80 °C, 10 mmHg). Yield: 0.20 g (50%). Mp: 120 °C. ^1H NMR (200 MHz) ($CDCl_3$): δ = 4.85 (t, 4H, Cp), 4.72 (t, 4H, Cp), 0.27 ppm (s, 12H, Si—Me). ^{13}C NMR ($CDCl_3$): δ = 71.0 (ipso, Cp), 76.8, 74.5 (α and β Cp), −0.15 ppm (Me). ^{29}Si NMR (C_6D_6): δ = −12.4 ppm. MS (EI, 70 eV): *m/z* 346 (M^+, 100%), in good agreement with isotopic abundance calculations. Anal. Calc: C, 48.7; H, 5.8. Found: C, 48.1; H, 5.9. UV/vis (THF): λ_{max} = 318 (ϵ = 232 M^{-1} cm^{-1}), 266 nm (ϵ = 290 M^{-1} cm^{-1}).

Attempted ROP of 6. (a) Samples of **6** (ca. 0.5 g 1.4 mmol) were heated in evacuated, sealed Pyrex glass tubes at temperatures of (i) 150 °C, (ii) 200 °C, (iii) 250 °C, and (iv) 350 °C for 7 days and (v) 380 °C for 15 min. No increase in melt viscosity was noted and the tube contents (dissolved in $CDCl_3$) were found to contain only unreacted **6** by ^1H NMR in the case of (i)—(iv). In the case of (v) partial decomposition of **6** resulting in the formation of insoluble black material was noted. ^1H NMR spectra of the soluble contents of this tube showed only unreacted **6**. In addition, analysis of the tube contents by mass spectrometry and GPC in THF showed that no high molecular weight (M_w > 1000) oligomeric or polymeric material was present.

(b) Samples of **6** (ca. 0.4 g, 1 mmol) together with ca. 1 mg (ca. 1 mol %) of K[$OSiMe_3$] were heated in evacuated sealed Pyrex glass tubes at (i) 140 °C for 1 h, (ii) 160 °C for 20 h, (iii) 220 °C for 5 h, and (iv) 350 °C for 72 h. In all cases no increase in melt viscosity was observed, and the tube contents (dissolved in $CDCl_3$) were subsequently found to contain only unreacted **6** by ^1H NMR. In addition, analysis by mass spectrometry and GPC showed that no high molecular weight (M_w > 1000) oligomeric material was present.

Synthesis of the [2][2]Ruthenocenophane 7. A solution of $Li_2[C_5H_3(SiMe_2)_2]_2$ (0.56 g, 1.5 mmol) in THF (40 mL) was added dropwise to a suspension of *cis*-$RuCl_2(DMSO)_4$ (0.75 g, 1.5 mmol) in the same solvent (40 mL) at −78 °C. The reaction mixture was stirred at this temperature for 3 h and was then allowed to warm to room temperature over a 12-h period. Following solvent removal in vacuo, pale-yellow microcrystalline **7** was isolated and purified by vacuum sublimation (85 °C, 10 mmHg). Yield: 0.35 g (51%). Mp: 130 °C. ^1H NMR (200 MHz) ($CDCl_3$): δ = 5.05 (d, 4H, $^3J_{HH}$ = 8 Hz, Cp), 4.87 (t, 2H, $^3J_{HH}$ = 8 Hz, Cp), 0.60 (s, 12H, Si—Me), 0.49 ppm (s, 12H, Si—Me). ^{13}C NMR ($CDCl_3$): δ = 71.0 (ipso, Cp), 82.5, 76.0 (α and β Cp), 4.05 (Me), 0.92 ppm (Me). ^{29}Si NMR (C_6D_6): δ = −11.1 ppm. MS (EI, 70 eV): *m/z* 460 (M^+, 100%), in good agreement with isotopic abundance calculations. Anal. Calc: C, 47.1; H, 6.5. Found: C, 47.4; H, 8.1. UV/vis (THF): λ_{max} = 345 (ϵ = 275 M^{-1} cm^{-1}), 270 nm (ϵ = 280 M^{-1} cm^{-1}).

Attempted ROP of 7. (a) Samples of **7** (ca 0.2 g, 0.4 mmol) were heated in evacuated, sealed Pyrex glass tubes at temperatures of (i) 150 °C, (ii) 200 °C, (iii) 250 °C, and (iv) 350 °C for 7 days and 380 °C for 15 min. In the case of tubes (i)—(iv), no increase in melt viscosity was noted and the tube contents (dissolved in $CDCl_3$) were found to contain only unreacted **6** by ^1H NMR. Heat treatment of **7** in an evacuated tube at 380 °C for 15 min resulted in the decomposition of the material and the formation of an insoluble black product. ^1H NMR

(21) Mercer, A.; Trotter, J. *J. Chem. Soc., Dalton Trans.* **1975**, 2480.

spectra of the contents of this tube showed only small amounts of unreacted **7**. In addition, analysis of the soluble tube contents by GPC in THF and mass spectrometry showed that no high molecular weight (M_w > 1000) oligomeric material was present.

(b) Ca. 0.2-g (0.4-mmol) samples of **7** together with ca. 1 mg (ca. 1 mol %) of K[OSiMe$_3$] were heated in evacuated sealed Pyrex glass tubes at (i) 140 °C for 1 h, (ii) 160 °C for 20 h, and (iii) 250 °C for 24 h. In cases (i)–(ii) no increase in melt viscosity was observed, and the tube contents (dissolved in $CDCl_3$) were subsequently found to contain only unreacted **7** by ^{1}H NMR. In addition, analysis by GPC and mass spectrometry showed that no high molecular weight (M_w > 1000) oligomeric or polymeric material was present. In the case of (iii) heat treatment at 250 °C resulted in the decomposition of **7** with the formation of brown insoluble material. Analysis of the soluble tube contents by NMR, mass spectrometry, and GPC showed no evidence for the formation of oligomers or polymers derived from **7**.

X-ray Structural Determination Technique. In what follows for **6**, details for **7** appear in parentheses. Intensity data were collected on an Enraf-Nonius CAD4 (Siemens P4) diffractometer at room temperature (185 K) using graphite monochrominated Mo Kα radiation, λ = 0.710 73 Å. The ω scan technique was used with variable scan speeds. For each structure the intensities of three standard reflections which were measured every 2 h (100 reflections) indicated no decay. The data were corrected for Lorentz and polarization effects and also for absorption.[22,(23)] The structures were solved by direct methods. Non-hydrogen atoms were refined with anisotropic thermal parameters by full-matrix least squares to minimize $\Sigma w(F_o - F_o)^2$, where $w^{-1} = \sigma_2(F_o) + g(F_o)^2$. For **6**, hydrogen atoms were positioned on geometric grounds with a C–H distance of 0.96 and were included in the refinement as riding atoms refined with isotropic thermal parameters. The hydrogen atoms of **7** were refined with isotropic thermal parameters. Crystal data, data collection, and least squares parameters are listed in Table 1. All calculations were performed and structural diagrams created using SHELXTL PC[22] on a 486 personal computer.

Acknowledgment. This work was supported by the Petroleum Research Fund (PRF) administered by the American Chemical Society and the Natural Science and Engineering Research Council of Canada (NSERC). We also thank the University of Toronto for an Open Fellowship and a Simcoe Fellowship for J.M.N., Mr. Nick Plavac for obtaining the ^{29}Si NMR spectra, and Johnson Matthey for a generous loan of ruthenium salts. In addition, I.M. is grateful to the Alfred P. Sloan Foundation for a Fellowship (1994–96).

Supplementary Material Available: Atomic coordinates, complete bond lengths and angles, anisotropic thermal parameters, hydrogen atom coordinates, and least squares plane data and figures showing the molecular structures (13 pages). Ordering information is given on any current masthead page.

OM940365Q

(22) Sheldrick, G. M. *SHELXTL PC*; Siemens Analytical X-ray Instruments, Inc.: Madison, WI, 1989.

(23) Sheldrick, G. M. SHELXA, Program for absorption correction, 1993 (in preparation for *J. Appl. Crystallogr.*).